Computers and Structures 325 (2026) 108167

Contents lists available at ScienceDirect

Computers and Structures

journal homepage: www.elsevier.com/locate/cas

Practical computation of initial sensitivities in dynamics of flexible multibody systems

Juan C. García Orden [a,*], Juan J. Arribas Montejo [b], Álvaro López Varela [c]

[a] Center for Intelligent and Sustainable Infrastructure (CIVILis), Escuela Técnica Superior de Ingenieros de Caminos, Canales y Puertos, Universidad Politécnica de Madrid, Calle Profesor Aranguren 3, 28040, Madrid, Spain

[b] Escuela Técnica Superior de Ingenieros de Caminos, Canales y Puertos, Universidad Politécnica de Madrid, Calle Profesor Aranguren 3, 28040, Madrid, Spain

[c] Laboratorio de Ingeniería Mecánica, Campus Industrial de Ferrol, CITENI.Universidade da Coruna, Mendizábal S/N, 15403, Ferrol, Spain

HIGHLIGHTS

- Systematic method presented for computing initial sensitivities in rigid and flexible systems.
- Flexible components are rigidized if initially undeformed in a Perturbed Initial Model (PIM).
- Initial sensitivities severely impacts the evolution of sensitivities and potentially optimization results.
- Formulation provided to handle flexible components treated as rigid in PIMs.

ARTICLE INFO

Keywords:
Flexible multibody systems
Sensitivity analysis
Initial sensitivities
Gradient-based optimization
Dynamics

ABSTRACT

Design optimization is a critical aspect in the development of mechanical systems, particularly flexible multibody systems, to enhance performance metrics such as weight reduction, efficiency, and cost-effectiveness. Gradient-based optimization methods are often employed for this purpose due to their computational efficiency, especially for large design spaces. These methods rely heavily on accurate sensitivity analysis, which involves computing the derivatives of system responses with respect to design parameters. While significant research exists on sensitivity analysis for the full dynamic trajectory of multibody systems, details the computation of the initial position and velocity sensitivities is a crucial step and is scarcely documented, being treated as an implementation detail. This paper highlights the importance of computing these initial sensitivities and presents a specific proposal for their systematic computation within the context of flexible multibody dynamics.

1. Introduction

Multibody System (MBS) dynamics is a fundamental area of research with applications spanning robotics, aerospace, automotive, and biomechanics [1]. The inclusion of flexibility in MBS models, leading to Flexible Multibody Systems (FMBS), is essential for accurate simulations of high-speed and lightweight mechanisms where elastic deformations are significant. The dynamic behavior of FMBS is complex, often modeled using differential-algebraic equations (DAEs), which capture the interplay between rigid body motion and structural deformation [2–4].

On the other hand, optimization of mechanical systems is essential for achieving improved designs in many applications, leading to outcomes such as reduced weight, increased efficiency, and lower costs. This optimization typically involves defining an objective function that depends on the system's dynamic response. Gradient-based optimization algorithms require computation of the gradient of the objective function with respect to design variables and can be performed using different techniques. One of them is numerical, with finite differences, solving the dynamics of several perturbed problems. This approach is simple and systematic but has some important drawbacks; namely, the selection of the perturbation, the low accuracy, and efficiency, especially when dealing with large systems and a large number of design variables. The other approach, which is the one adopted in this paper, is through a sensitivity analysis that evaluates how the system's output changes in response to variations in design parameters. Efficient sensitivity analysis is the cornerstone of efficient gradient-based optimization.

Common methods for sensitivity analysis in multibody dynamics include the Direct Differentiation Method (DDM) and the Adjoint Variable Method (AVM). The DDM involves differentiating the equations of

* Corresponding author.
Email address: juancarlos.garcia@upm.es (J.C. García Orden).

https://doi.org/10.1016/j.compstruc.2026.108167
Received 11 September 2025; Accepted 24 February 2026
Available online 9 March 2026

motion directly with respect to the design parameters and solving the resulting sensitivity equations forward in time, coupled with or after the original (primal) dynamic equations. The AVM, in contrast, introduces adjoint variables and solves a backward-in-time system of adjoint equations, offering computational efficiency benefits, especially when the number of design parameters is large compared to the number of objective functions or constraints. The derivatives involved in both DDM and AVM can be performed analytically, numerically, or with automatic differentiation [5]. Reference [6] describes a very efficient implementation of these techniques, applied to academic and practical engineering examples, especially when a large number of design variables is involved.

Regardless of the specific sensitivity method, the accurate computation of the sensitivities over the entire time history of the dynamic response depends on the initial conditions of the sensitivity equations. These initial sensitivities represent the derivatives of the initial state (initial positions and velocities) with respect to the design parameters. Although critical for initiating the time integration of the sensitivity equations and thus obtaining accurate gradients for optimization, the computation of these initial sensitivities is often considered an implementation detail in the literature [5,7,8] and is not fully detailed.

Flexible bodies introduce additional degrees of freedom whose initial sensitivities have to be defined somehow. In many cases, the computation of their initial values is not an issue, since the parameters are not relevant to them (e.g., the sensitivity of initial positions and velocities with respect to material properties, or particular geometric parameters); in these cases, which appear in many of the popular examples found in the literature, sensitivities can be assumed to be null [8–13]. This issue will be discussed further in Section 3.

In cases where these initial sensitivities are foreseeing to be not null, a common and simple approach is to consider initially rigid deformable bodies [7,9], without fully explain the motivation and applicability. Indeed, this choice naturally appears when a floating frame of reference (FFR) is employed, since the floating frame directly enforces the initial rigid-body kinematics (rigid translations and rotations) [14]. But the situation is not so simple when absolute coordinates are employed, as is the case when using finite elements with a fully nonlinear formulation, for instance. In this case, this approach requires specialized formulations that are typically omitted from the literature. Although these formulations are quite simple, their careful development and implementation are crucial.

This paper focuses on these key aspects and presents a specific proposal for the systematic analysis of the initial sensitivity computation for FMBS dynamics. To the best of the author's knowledge, despite its importance, such a systematic attempt has not been reported in the literature.

The outline of the paper is as follows. Section 2 describes the general setup of the sensitivity analysis in Multibody Dynamics. Section 3 discusses the relevance and complexity of the calculation of initial sensitivities, both from purely rigid to deformable MBS, while Section 4 proposes a simple procedure for including initially rigid flexible bodies. Finally, Section 5 draws some final conclusions.

2. Sensitivity analysis in multibody dynamics

Let us consider a flexible MBS parametrized with n coordinates and velocities grouped in vectors $\boldsymbol{q}$ and $\dot{\boldsymbol{q}} \in \mathbb{R}^n$. These coordinates could be diverse: positions and slopes at selected points (as in the ANCF formulation), Cartesian absolute coordinates of points and unit vectors (natural coordinates), or just Cartesian absolute coordinates of points (as employed in isoparametric finite elements). Coordinates $\boldsymbol{q}$ could be dependent through a set of holonomic constraints $\boldsymbol{\Phi}(\boldsymbol{q}, t) \in \mathbb{R}^m$. Employing the notation $(\cdot)_{\square} = \partial(\cdot)/\partial\square$, the equations of motion of such a system are expressed by the index−3 DAE system:

$$\boldsymbol{M}\ddot{\boldsymbol{q}} + \boldsymbol{\Phi}_{\boldsymbol{q}}^{\mathrm{T}}\lambda = \boldsymbol{Q}, \quad \boldsymbol{\Phi} = \boldsymbol{0} \quad + \quad \text{initial conditions } \boldsymbol{q}_0, \dot{\boldsymbol{q}}_0, \lambda_0 \tag{1}$$

$\boldsymbol{M}$ being the $n\times n$ mass matrix, $\lambda \in \mathbb{R}^m$ being a set of Lagrange multipliers and $\boldsymbol{Q} \in \mathbb{R}^n$ a vector grouping the external forces plus possible velocity dependent inertia forces. For certain types of coordinates (e.g., Cartesian absolute coordinates of selected points), these velocity dependent inertia forces could be null and therefore the mass matrix could be constant. The system represented by (1) has $d = n-r$ Degrees of Freedom (DOFs), being $r = rank(\boldsymbol{\Phi}_{\boldsymbol{q}})$. In what follows, we will consider that these constraints are independent, thus $r = m$.

On the other hand, let us consider a parameter $\rho \in \mathbb{R}$, which can be diverse too: geometric (may be a distance, etc.) or constitutive (the stiffness of a spring, material properties of the material a flexible body is made of, etc.). The consideration of several parameters simultaneously with a vector $\boldsymbol{\rho} \in \mathbb{R}^p$ with $p > 1$ is perfectly possible but obscures the mathematical expressions to be considered without adding a valuable insight to the proposal. What is more, we will assume that the initial conditions $\boldsymbol{q}_0, \dot{\boldsymbol{q}}_0$ and λ_0 in (1) are given and are not parameters of the problem.

Sensitivity analysis is usually the initial stage of an optimization process of a dynamical system, looking for the stationary point of an objective functional ψ, with the general expression:

$$\psi(\boldsymbol{q}(t), \dot{\boldsymbol{q}}(t), \ddot{\boldsymbol{q}}(t), \lambda(t), \rho) = \int_{t_0}^{t_F} g(\boldsymbol{q}, \dot{\boldsymbol{q}}, \ddot{\boldsymbol{q}}, \lambda, \rho)\, \mathrm{d}t \tag{2}$$

This problem is typically solved employing a gradient method, that requires the computation of the derivative of the funcional with respect to the parameter; applying the chain rule:

$$\psi_\rho = \int_{t_0}^{t_F} \left[g_{\boldsymbol{q}}\boldsymbol{q}_\rho + g_{\dot{\boldsymbol{q}}}\dot{\boldsymbol{q}}_\rho + g_{\ddot{\boldsymbol{q}}}\ddot{\boldsymbol{q}}_\rho + g_\lambda \lambda_\rho + g_\rho\right]\, \mathrm{d}t, \tag{3}$$

where $\boldsymbol{q}_{\rho(t)}, \dot{\boldsymbol{q}}_\rho(t), \ddot{\boldsymbol{q}}_\rho(t) \in \mathbb{R}^n$ and $\lambda_\rho(t) \in \mathbb{R}^m$ are the sensitivities of $\boldsymbol{q}(t), \dot{\boldsymbol{q}}(t), \ddot{\boldsymbol{q}}(t)$ and $\lambda(t)$ respectively. In the direct approach (DDM) these sensitivities are obtained by solving the so-called Tangent Linear Model, which results from taking the derivative of the equations of motion (1) with respect to the parameter:

$$\boldsymbol{M}\ddot{\boldsymbol{q}}_\rho + \hat{\boldsymbol{C}}\dot{\boldsymbol{q}}_\rho + \hat{\boldsymbol{K}}\boldsymbol{q}_\rho + \boldsymbol{\Phi}_{\boldsymbol{q}}^{\mathrm{T}}\lambda_\rho = \hat{\boldsymbol{Q}}, \qquad \boldsymbol{\Phi}_{\boldsymbol{q}}\boldsymbol{q}_\rho + \boldsymbol{\Phi}_\rho = \boldsymbol{0}$$
$$+ \quad \text{initial conditions } \boldsymbol{q}_{\rho_0}, \dot{\boldsymbol{q}}_{\rho_0}, \lambda_{\rho_0} \tag{4}$$

which is a linear differential system with time-dependent coefficients $\boldsymbol{M}(\boldsymbol{q}(t), t)$, $\hat{\boldsymbol{C}}(\boldsymbol{q}(t), \dot{\boldsymbol{q}}(t), t)$, $\hat{\boldsymbol{K}}(\boldsymbol{q}(t), \dot{\boldsymbol{q}}(t), \ddot{\boldsymbol{q}}(t), \lambda(t), t)$, and $\hat{\boldsymbol{Q}}(\boldsymbol{q}(t), \dot{\boldsymbol{q}}(t), \ddot{\boldsymbol{q}}(t), \lambda(t), t)$. Their precise form can be found, for instance, in [15]. Note that constraints $\boldsymbol{\Phi}$ and their derivatives $\boldsymbol{\Phi}_{\boldsymbol{q}}, \boldsymbol{\Phi}_{\boldsymbol{q}\boldsymbol{q}}, \boldsymbol{\Phi}_{\boldsymbol{q}\rho}$ and $\boldsymbol{\Phi}_\rho$ are embedded in these terms.

The dynamic equations (1) and the sensitivity equations (4) are typically solved numerically using time integration schemes. The sensitivity analysis can be performed simultaneously or after the dynamic analysis.

3. The challenge of initial sensitivities

The time integration of the sensitivity equations (4) requires initial conditions for the sensitivities, which are critical for the accuracy of the sensitivity analysis over the entire time interval. While the overall framework in the context of DAEs is established, the practical steps and potential challenges in defining the correct starting values for the sensitivities are often not elaborated upon.

Constraints should always be satisfied for any value of ρ; for $t = 0$ too, such that the following identities must hold:

$$\left.\frac{\mathrm{d}\boldsymbol{\Phi}}{\mathrm{d}\rho}\right|_0 = \boldsymbol{0} \;\rightarrow\; \left.\left(\boldsymbol{\Phi}_{\boldsymbol{q}}\boldsymbol{q}_\rho\right)\right|_0 = \left.-\boldsymbol{\Phi}_\rho\right|_0 \tag{5}$$

$$\left.\frac{\mathrm{d}\dot{\boldsymbol{\Phi}}}{\mathrm{d}\rho}\right|_0 = \boldsymbol{0} \;\rightarrow\; \left.\left(\boldsymbol{\Phi}_{\boldsymbol{q}}\dot{\boldsymbol{q}}_\rho\right)\right|_0 = \left.\left(-(\boldsymbol{\Phi}_{\boldsymbol{q}}\boldsymbol{q}_\rho)_{\boldsymbol{q}}\dot{\boldsymbol{q}} - \boldsymbol{\Phi}_{t\boldsymbol{q}}\boldsymbol{q}_\rho - \boldsymbol{\Phi}_{\boldsymbol{q}\rho}\dot{\boldsymbol{q}} - \boldsymbol{\Phi}_{t\rho}\right)\right|_0 \tag{6}$$

Systems (5) and (6) have m equations each and allow to compute the initial sensitivities $\boldsymbol{q}_{\rho_0}$ and $\dot{\boldsymbol{q}}_{\rho_0}$ respectively, provided that $n = m$. However, this is not the case for most systems, which have $d = n - m \neq 0$ DOFs. What is more, flexible systems, as will be discussed in the next section, may require the addition of m_r special constraints $\boldsymbol{\Lambda}(\boldsymbol{q}) \in \mathbb{R}^{m_r}$, which when derived with respect to the parameter, provide two sets of equations similar to (5) and (6). These constraints are special in the sense that they are active just for $t = 0$, for the computation of the initial sensitivities.

Finally, in order to solve the expanded system that accounts for constraints $\boldsymbol{\Phi}$ and $\boldsymbol{\Lambda}$, additional $d_s = d - m_r$ equations must be added to select the remaining degrees of freedom which we denote as Sensitivity Degrees of Freedom (SDOFs). In order to do this, it is necessary first to define a set of coordinates $\boldsymbol{z}(\boldsymbol{q}) \in \mathbb{R}^{d_s}$ that will represent these SDOFs, through a general set of d_s nonlinear independent equations. These, derived with respect to the parameter, provide the required additional two sets of d_s equations:

$$\left.\frac{\mathrm{d}z}{\mathrm{d}\rho}\right|_0 = \boldsymbol{z}_{\rho_0} \quad \rightarrow \quad \left(\boldsymbol{z}_{\boldsymbol{q}}\boldsymbol{q}_{\rho}\right)\Big|_0 = \boldsymbol{z}_{\rho_0}$$

$$\left.\frac{\mathrm{d}\dot{z}}{\mathrm{d}\rho}\right|_0 = \dot{\boldsymbol{z}}_{\rho_0} \quad \rightarrow \quad \left(\boldsymbol{z}_{\boldsymbol{q}}\dot{\boldsymbol{q}}_{\rho} + (\boldsymbol{z}_{\boldsymbol{q}}\boldsymbol{q}_{\rho})_{\boldsymbol{q}}\dot{\boldsymbol{q}}\right)\Big|_0 = \dot{\boldsymbol{z}}_{\rho_0} \tag{7}$$

where their initial values have been collected in vectors $\boldsymbol{z}_{\rho_0}$ and $\dot{\boldsymbol{z}}_{\rho_0} \in \mathbb{R}^{d_s}$. The global systems can be written in compact form:

$$\boldsymbol{A}\boldsymbol{q}_{\rho_0} = \begin{Bmatrix} -\boldsymbol{\Phi}_{\rho_0} \\ -\boldsymbol{\Lambda}_{\rho_0} \\ \boldsymbol{z}_{\rho_0} \end{Bmatrix} \tag{8}$$

$$\boldsymbol{A}\dot{\boldsymbol{q}}_{\rho_0} = \begin{Bmatrix} -(\boldsymbol{\Phi}_{\boldsymbol{q}_0}\boldsymbol{q}_{\rho_0})_{\boldsymbol{q}_0}\dot{\boldsymbol{q}}_0 - \boldsymbol{\Phi}_{t\boldsymbol{q}_0}\boldsymbol{q}_{\rho_0} - \boldsymbol{\Phi}_{\boldsymbol{q}\rho_0}\dot{\boldsymbol{q}}_0 - \boldsymbol{\Phi}_{t\rho_0} \\ -(\boldsymbol{\Lambda}_{\boldsymbol{q}_0}\boldsymbol{q}_{\rho_0})_{\boldsymbol{q}_0}\dot{\boldsymbol{q}}_0 \\ -(\boldsymbol{z}_{\boldsymbol{q}_0}\boldsymbol{q}_{\rho_0})_{\boldsymbol{q}_0}\dot{\boldsymbol{q}}_0 + \dot{\boldsymbol{z}}_{\rho_0} \end{Bmatrix} \tag{9}$$

which are two systems of n algebraic linear equations each, sharing the same coefficient matrix $\boldsymbol{A}$ of size $n \times n$:

$$\boldsymbol{A} = \begin{pmatrix} \boldsymbol{\Phi}_{\boldsymbol{q}_0} \\ \boldsymbol{\Lambda}_{\boldsymbol{q}_0} \\ \boldsymbol{z}_{\boldsymbol{q}_0} \end{pmatrix} \tag{10}$$

Solving (8) and (9) for $\boldsymbol{q}_{\rho_0}$ and $\dot{\boldsymbol{q}}_{\rho_0}$ respectively, vectors $\ddot{\boldsymbol{q}}_{\rho_0}$ and λ_{ρ_0} can be computed through the dynamic sensitivities, see [16].

Remark 3.1. The $d_s \times n$ matrix $\boldsymbol{z}_{\boldsymbol{q}_0}$ is often denoted as $\boldsymbol{B}$ [16,17]. Note that if $\boldsymbol{z}(\boldsymbol{q})$ is linear, matrix $\boldsymbol{z}_{\boldsymbol{q}_0}$ does not depend on $\boldsymbol{q}_0$ and $\boldsymbol{z}_{\boldsymbol{q}\boldsymbol{q}_0}$ is null, and the final systems (8) and (9) in this case take a simpler form. Furthermore, note that if the SDOFs are a subset of the DOFs, matrix $\boldsymbol{z}_{\boldsymbol{q}_0}$ is Boolean.

It is very important to note that the presence of deformable parts may cause the number of SDOFs to be different from the number of DOFs ($d_s \neq d$). Furthermore, the specific identification of the SDOFs of the problem, defined by $\boldsymbol{z}(\boldsymbol{q})$ (and consequently matrix $\boldsymbol{z}_{\boldsymbol{q}_0}$), and their associated initial sensitivity values $\boldsymbol{z}_{\rho_0}$ and $\dot{\boldsymbol{z}}_{\rho_0}$ may not be unique and are crucial to the process.

In this context, it is handy to introduce the concept of Perturbed Initial Model (PIM). For a given parameter, each PIM leads to different sensitivity results through the related initial sensitivity conditions. Specifically, a PIM is defined as a mechanical model with the following characteristics:

- It is only defined at $t = 0$.
- It is identical to the original system but incorporates a variation of the selected parameter.
- It incorporates m_r additional constraints $\boldsymbol{\Lambda}(\boldsymbol{q}) \in \mathbb{R}^{m_r}$ to the original ones $\boldsymbol{\Phi}(\boldsymbol{q}) \in \mathbb{R}^m$ when flexible bodies are present and are considered initially undeformed.
- It has $d_s = d - m_r$ degrees of freedom named Sensitivity Degrees of Freedom (SDOFs).

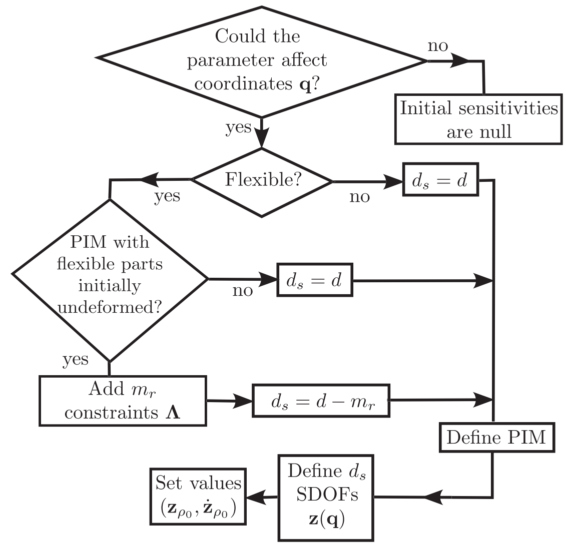

Fig. 1. Workflow for the calculation of initial sensitivities.

Note that the concept of a PIM naturally emerges when evaluating the sensitivities with a finite-difference technique, but could be overlooked when using analytical approaches. It is important to stress that the utility of the PIM does not extend beyond $t = 0$, and may incorporate constraints additional to those of the original system. Observe that the initial sensitivities are obtained by solving systems (8) and (9) provided the analyst defines d_s initial sensitivities, typically motivated for practical physical reasons (e.g, operational limitations of the experimental setup, etc.), thus choosing among different possible PIMs.

Based on the previous concepts, the general workflow for the calculation of the initial sensitivities is shown in Fig. 1. Note that the first relevant aspect is to evaluate whether a variation in the parameter could affect any of the coordinates $\boldsymbol{q} \in \mathbb{R}^n$ of the model. If there is no effect, the initial sensitivities are null and no further calculation is necessary. This would be the case, for instance, when the parameter is not geometric (such as the elastic modulus of the material of a flexible body) or affects the internal geometry (such as the section of a bar or the natural length of a spring).

Next sections will illustrate these concepts for both rigid and flexible systems with particular examples, assuming from the start that the parameter could affect the coordinates and, therefore, the calculation of the initial sensitivities is not trivial.

3.1. Rigid MBS

We conceive a rigid MBS as composed only by rigid bodies. Discrete springs and dampers will be considered a special class of deformable bodies, with no inertia, and therefore excluded from these systems. In addition, we will assume that the initial conditions $\boldsymbol{q}_0$ and $\dot{\boldsymbol{q}}_0$ of the dynamic problem are given and are not parameters. As explained in the previous Section, no additional constraints $\boldsymbol{\Lambda}$ are necessary in this type of system, and thus the PIMs have the same SDOFs (d_s) as DOFs of the original model (d).

To illustrate the analysis, we will employ the representative example of the five-bar mechanism [18–20] shown in Fig. 2, with $k_1 = k_2 = 0$. The masses are $m_{A-1} = m_{3-B} = 1$ kg and $m_{1-2} = m_{2-3} = 1.5$ kg. The model is contained in the fixed vertical plane XZ and it is released from rest under the action of gravity $g = 9.81$ m/s^2. In the 2D space, the model is represented by the $n = 3 \times 2 = 6$. Cartesian coordinates of points $1, 2, 3$ grouped in the vector $\boldsymbol{q} = (x_1, z_1, x_2, z_2, x_3, z_3)^{\mathrm{T}} \in \mathbb{R}^6$ that are related by a set of $m = 4$ independent constraints that enforce the constant distances between A-1, 1-2, 2-3 and 3-B. Thus, the model has $d = n - m = 6 - 4 = 2$ DOFs and the same number d_s of SDOFs.

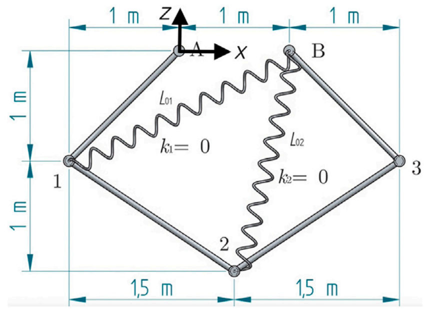

Fig. 2. Five-bar mechanism, adapted from [18].

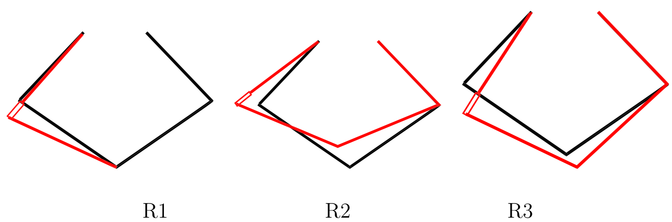

Fig. 3. Rigid MBS. Three different possible PIMs, all with $n_s = n$. Incremental L_{A1} represented by a hollow segment.

As explained previously, the user must define the SDOFs and define its initial values providing equations (7). The definition of SDOFs should be based on physical reasons, depending on how the system would be perturbed in reality, and it will be associated with an specific PIM. We will illustrate the situation with the example, computing the sensitivity of the vertical position of the point 2 with respect to the length of the bar A-1, denoted by L_{A1}. We will assume that $\dot{z}_{\rho_0} = \mathbf{0}$ and, in consequence, system (9) stablishes that the initial sensitivity velocities $\dot{q}_{\rho_0}$ are null, since $\boldsymbol{\Phi}_t = \mathbf{0}$ and $\dot{q}_0 = \mathbf{0}$. Among many, the three different PIMs of Fig. 3 may be considered:

R1. The points 2 and 3 keep their positions. As a consequence, point 1 is initially displaced to accommodate the perturbed length L_{A1}. One choice for vector $z(q)$ is:

$$z(q) = \left\{ \begin{array}{c} z_2 \\ x_3 \end{array} \right\} \rightarrow z_{q_0} = \left(\begin{array}{cccccc} 0 & 0 & 0 & 1 & 0 & 0 \\ 0 & 0 & 0 & 0 & 1 & 0 \end{array} \right), z_{\rho_0} = \left\{ \begin{array}{c} 0 \\ 0 \end{array} \right\} \tag{11}$$

that identifies (z_2, x_3) as the SDOFs and set their initial sensitivities to null. Note that in this case the SDOFs are a subset of the DOFs, so matrix z_{q_0} is Boolean. The detailed equations and the solution is presented in Appendix A.1.

R2. Point 3 keeps its position and point 1 is horizontally displaced. As a consequence, as seen in Fig. 3, point 2 should move upwards and leftwards to accommodate the perturbed length A-1. This means that the initial sensitivity of its vertical position will be positive. One choice for vector $z(q)$ is:

$$z(q) = \left\{ \begin{array}{c} z_1 \\ x_3 \end{array} \right\} \rightarrow z_{q_0} = \left(\begin{array}{cccccc} 0 & 1 & 0 & 0 & 0 & 0 \\ 0 & 0 & 0 & 0 & 1 & 0 \end{array} \right), z_{\rho_0} = \left\{ \begin{array}{c} 0 \\ 0 \end{array} \right\} \tag{12}$$

R3. Point 3 keeps its position and point 1 is initially vertically displaced. As a consequence, as seen in Fig. 3, point 2 should move downwards and rightwards to accommodate the perturbed length A-1. This means that the initial sensitivity of its vertical position will be negative. One choice for vector $z(q)$ is:

$$z(q_0) = \left\{ \begin{array}{c} x_1 \\ x_3 \end{array} \right\} \rightarrow z_{q_0} = \left(\begin{array}{cccccc} 1 & 0 & 0 & 0 & 0 & 0 \\ 0 & 0 & 0 & 0 & 1 & 0 \end{array} \right), z_{\rho_0} = \left\{ \begin{array}{c} 0 \\ 0 \end{array} \right\} \tag{13}$$

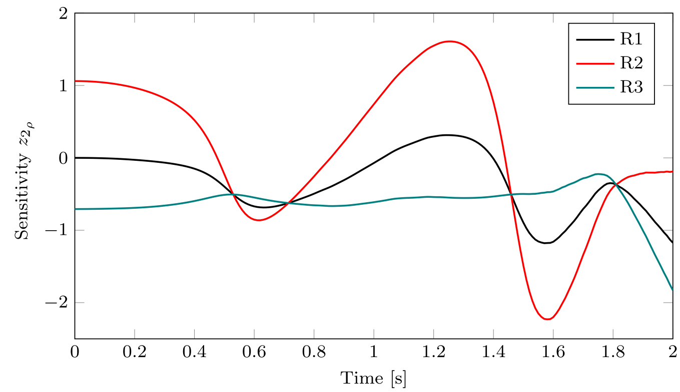

Fig. 4. Five bar mechanism without springs. Sensitivity of the vertical coordinate of point 2respectL_{A1}(length of bar $A-1$).

Fig. 4 shows that Equations (8) sets different values for the initial sensitivity for each case, producing a completely different evolution of the sensitivity over time.

3.2. Flexible MBS: five-bar mechanism

The presence of flexible bodies substantially affects how the different PIMs should be defined. To illustrate this situation, we will consider the five-bar mechanism of the previous example but incorporate massless linear springs between points B-1 and B-2 and an elastic beam, with the formulation described in [21,22], which replaces bar 1-2, discretized in two segments as shown in Fig. 5. Any other beam model could be incorporated without loss of generality. The natural lengths of the springs are such that both are, for the nominal dynamic problem, initially unloaded, and the beam 1-2, with elastic constants $E = 206.94$ GPa and $\nu = 0.288$, is initially undeformed. Due to its specific formulation, the discretization of the beam in two segments just adds the two Cartesian coordinates of the midpoint 4, such that $q = (x_1, z_1, x_2, z_2, x_3, z_3, x_4, z_4)^{\mathrm{T}} \in \mathbb{R}^8$ and the dynamics has $d = n - m = 8 - 3 = 5$ DOFs. The cross section of the beam is a square with side of 0.01031 m and the density of the material is 7829.0 kgm^{-3}, which provides the same mass as the rigid bar.

In this case, d_s could be different from d if some of the flexible bodies are initially undeformed. The situation will be illustrated by the five-bar mechanism of Fig. 5, with the objective of performing a sensitivity analysis of the vertical coordinate of the point 2. Among many, we will consider 6 different PIMs depicted in Figs. 6 and 8:

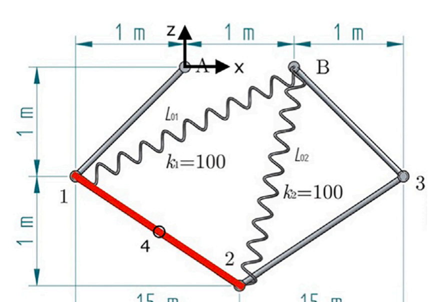

Fig. 5. Flexible five-bar mechanism, adapted from [18].

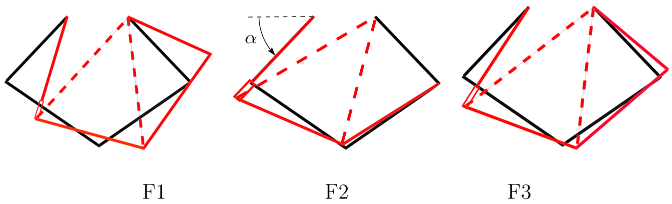

Fig. 6. Flexible MBS. Parameter L_{A1}. Three possible different PIMs. Incremental L_{A1} represented by a hollow segment. $n_s \leq n$.

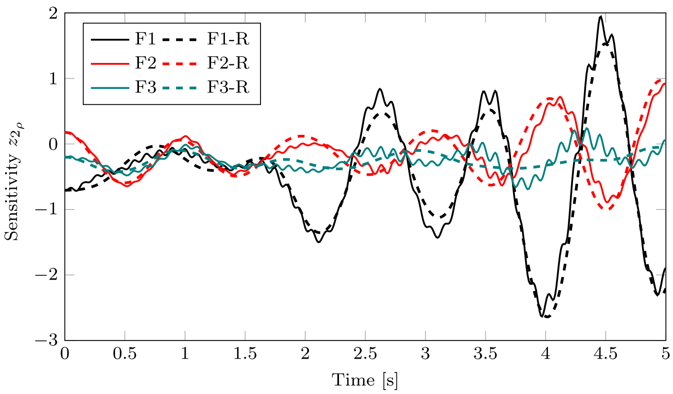

Fig. 7. Flexible five bar mechanism. Sensitivity of the vertical coordinate of point 2 respect to L_{A1}. F: flexible 1–2 bar; R: rigid 1–2 bar.

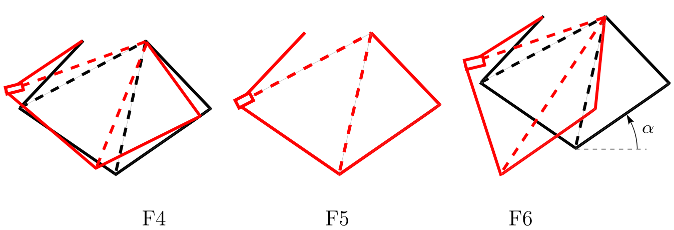

Fig. 8. Flexible MBS. Parameter L_{B1}. Three possible different PIMs. Incremental L_{B1} represented by a hollow segment. $n_s \leq n$.

- Cases F1, F2 and F3 where the parameter belongs to a rigid body; specifically, the length of the bar A-1 (L_{A1}), which was considered in R1, R2 and R3 too.
- Cases F4, F5 and F6 where the parameter belongs to a deformable part; specifically, the natural length of the spring B-1 (L_{B1}).

F1. The PIM incorporates the flexible bodies (bar 1–2 and both springs) undeformed. Thus, five more constraints $\boldsymbol{\Lambda} \in \mathbb{R}^5$ should be added (three for the beam and one for each spring), such that $d_s = d - m_r = 5 - 5 = 0$ which means that the user can not define any SDOFs; all of them are initially set. This makes sense: if we materialize the PIM with rigid bars and undeformed springs, the geometry is fully determined, with no option for user intervention. In fact, adding a new spring of arbitrary natural length (e.g., from A to 2) would make impossible to materialize the perturbed system with all the springs undeformed. Thus, $\boldsymbol{z}(\boldsymbol{q}), \boldsymbol{z}_{q_0}$ and $\boldsymbol{z}_{\rho_0}$ are absent from the formulation. Details are presented in Appendix A.2.

F2. In this PIM only bar 1–2 is initially undeformed; therefore three constaints $\boldsymbol{\Lambda}(\boldsymbol{q}) \in \mathbb{R}^3$ should be added, such that the number of SDOFs is $d_s = 5 - 3 = 2$. These SDOFs are defined assuming that point 3 initially keeps its position, and the angle α between bar 1–2 and the horizontal is maintained:

$$\boldsymbol{z}(\boldsymbol{q}) = \left\{ \begin{array}{c} x_3 \\ \arctan(z_1/x_1) \end{array} \right\}$$

$$\boldsymbol{z}_{q_0} = \begin{pmatrix} 0 & 0 & 0 & 0 & 1 & 0 & 0 & 0 \\ -\frac{z_{1_0}}{x_{1_0}^2 + z_{1_0}^2} & \frac{x_{1_0}}{x_{1_0}^2 + z_{1_0}^2} & 0 & 0 & 0 & 0 & 0 & 0 \end{pmatrix},$$
$$\boldsymbol{z}_{\rho_0} = \left\{ \begin{array}{c} 0 \\ 0 \end{array} \right\} \tag{14}$$

F3. In this PIM beam 1–2 and spring B-2 are initially undeformed; therefore four constaints $\boldsymbol{\Lambda}(\boldsymbol{q}) \in \mathbb{R}^4$ should be added (three for the beam and one for the spring), such that the number of SDOFs is $d_s = 5 - 4 = 1$. This SDOF is defined assuming that point 1 is initially vertically displaced.

$$\boldsymbol{z}(\boldsymbol{q}) = \left\{ \; x_1 \; \right\}$$
$$\boldsymbol{z}_{q_0} = \begin{pmatrix} 1 & 0 & 0 & 0 & 0 & 0 & 0 & 0 \end{pmatrix}, \quad \boldsymbol{z}_{\rho_0} = \left\{ \; 0 \; \right\} \tag{15}$$

Fig. 7 shows that each case sets different values for the initial sensitivity, producing a completely different evolution of the sensitivity over time. The Figure also includes results for the system where the flexible bar 1–2 has been replaced by a rigid one. Is observed that it introduces a noticiable effect, specially in the case F3.

F4. The PIM incorporates the flexible bodies undeformed, similarly to F2, but in this case the parameter is the natural length L_{B1} of spring B-1. This causes the PIM to be qualitatively different, as can be observed comparing F1 and F4 in Figs. 6 and 8 respectively. Due to the five constraints $\boldsymbol{\Lambda}(\boldsymbol{q})$ to be added from beam and the springs, the number of SDOFs is $d_s = 5 - 5 = 0$, and $\boldsymbol{z}(\boldsymbol{q}), \boldsymbol{z}_{q_0}$ and $\boldsymbol{z}_{\rho_0}$ are absent from the formulation.

F5. In this PIM beam 1–2 and spring B-2 are initially undeformed; therefore four constaints $\boldsymbol{\Lambda}(\boldsymbol{q}) \in \mathbb{R}^4$ should be added (three for the beam and one for the spring), such that the number of SDOFs is $d_s = 5 - 4 = 1$. This SDOF is defined assuming that point 1 remains in its position. Note that, since the parameter is the natural length L_{B1} of spring B-1, this choice causes this spring to be initially deformed (prestressed). Furthermore, it causes that all points keep their initial positions; therefore, the initial sensitivities will result null. One choice for vector $\boldsymbol{z}(\boldsymbol{q})$ is:

$$\boldsymbol{z}(\boldsymbol{q}) = \left\{ \; x_1 \; \right\}$$
$$\boldsymbol{z}_{q_0} = \begin{pmatrix} 1 & 0 & 0 & 0 & 0 & 0 & 0 & 0 \end{pmatrix}, \quad \boldsymbol{z}_{\rho_0} = \{0\} \tag{16}$$

F6. In this PIM beam 1–2 and spring B-1 are initially undeformed; therefore four constaints $\boldsymbol{\Lambda}(\boldsymbol{q}) \in \mathbb{R}^4$ should be added (three for the beam and one for the spring), such that the number of SDOFs is $d_s = 5 - 4 = 1$. This SDOF is defined as the angle α of bar 2–3 respect to the horizontal:

$$\boldsymbol{z}(\boldsymbol{q}) = \left\{ \arctan((z_3 - z_2)/(x_3 - x_2)) \right\}$$
$$\boldsymbol{z}_{q_0} = a \Big(0 \quad 0 \quad (z_{3_0} - z_{2_0}) \quad -(x_{3_0} - x_{2_0}) \quad -(z_{3_0} - z_{2_0}) \quad (x_{3_0} - x_{2_0}) \quad 0 \quad 0 \Big)$$
$$\boldsymbol{z}_{\rho_0} = \left\{ \; 0 \; \right\} \tag{17}$$

with $a = 1/[(x_{3_0} - x_{2_0})^2 + (z_{3_0} - z_{2_0})^2]$.

Fig. 9 shows that each case sets different values for the initial sensitivity, which produces very different evolutions in time. As in Figs. 7and 9 also includes results for the system where the flexible bar 12 has been replaced by a rigid one.

All test cases are summarized in Table 1. Note that in the Perturbed Configuration column, assumptions regarding the initial configuration of the flexible parts are highlighted in red. The assumptions that allow the definition of the d_s SDOFs and their values are in standard black color.

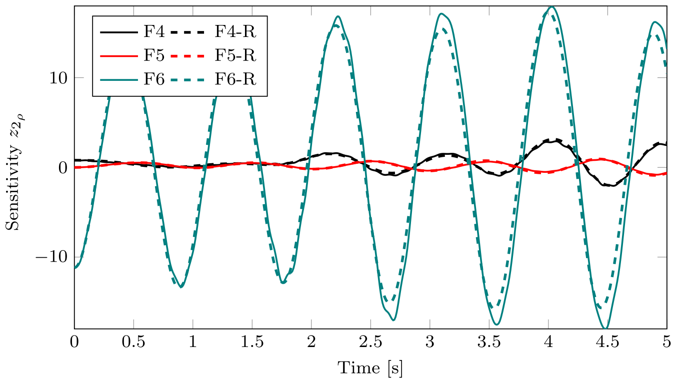

Fig. 9. Flexible five bar mechanism. Sensitivity of the vertical coordinate of point 2 respect to the natural length of spring $B1$. F: flexible 1–2 bar; R: rigid 1–2 bar.

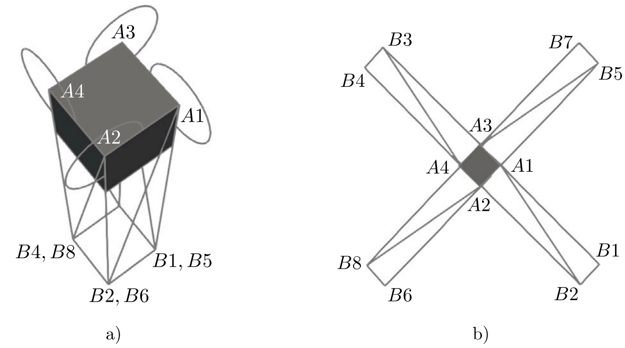

Fig. 10. Four-panel satellite: geometrical description. a) Perspective from the top, undeployed configuration; b) Plant view with the panels fully deployed.

3.3. Flexible MBS: Deployable space structure

We consider in this example a more complex mechanism, a flexible space deployable structure. The model consists of a rigid cubic body representing a satellite and a set of rigid and deformable beams representing the solar panels. The deployment maneuver relies on the effect of several initially deformed parts that are suddenly released from a locked position. These parts are four elastic beams that are straight in the undeformed state but are initially deformed in a circular shape, connecting the satellite body with four of the panel beams, acting as rotational springs.

Fig. 10(a) and (b) show a perspective from the top and a plan view of the satellite undeployed and fully deployed respectively. Fig. 10(a) allows to observe the configuration of the four springs, while Fig. 10(b) more clearly shows the structure of the panels.

The rotational springs are constrained to move in four different planes of the satellite body and are modeled by the same beam formulation employed in the previous example, with 20 segments each. The eight panel beams $A1-B1$, $A2-B2$, $A3-B3$, $A4-B4$, $A1-B5$, $A3-B7$, $A2-B6$ and $A4-B8$ are modeled with the same beam formulation and 10 segments each. The four bars $B1-B2$, $B3-B4$, $B5-B7$ and $B6-B8$ are rigid, and the four diagonals $A1-B2$, $A2-B8$, $A4-B3$ and $A3-B5$ are single beam segments that deform only axially. All joints $A1$ to $A4$ and $B1$ to $B8$ are spherical. Table 2 contains a summary of the geometric and material properties of the model.

Fig. 11 shows some snapshots of the movement during the first 5 s. The dynamics is integrated up to 10 s with a BDF-1 method time-step size $\Delta t = 0.02$ s. The geometry, elastic characteristics of the material and masses may not be very realistic but have been selected in order to define a complex model with visible large flexibility and with an affordable computational cost, using a very robust integrator that allows fairly large time-step sizes at the cost of significant numerical damping.

The model has 501 coordinates and a total of $d = 454$ DOFs. Let us consider the sensitivity of the position of the point $B2$ with respect to the length of the rigid bar $B1-B2$, and the definition of two different PIMs, SAT1 and SAT2. In both of them, all flexible bodies are initially undeformed except diagonal beam $A1-B2$, which implies the enforcement of additional $m_r = 447$ constraints and a total of $d_s = 7$ SDOFs $(x_G, y_G, z_G, \psi, \theta, \varphi, x_{B2})$: the first six correspond to the rigid-body DOFs of the complete satellite (position of the center of mass and orientation), and the last one corresponds to the out-of-the-panel-plane distance of $B2$ (the complete panel $A1-B1-B2-A1$ is initially contained in the $x = 0$ plane in the initial nominal undeployed configuration). What is more, let us assume that these 7 coordinates occupy the last positions in the global coordinate vector $\boldsymbol{q}$. Note that in both PIMs the diagonal $A1-B2$ is initially deformed (therefore, pre-stressed):

SAT1. In this PIM, the initial sensitivities of the position of the center of mass and orientation of the satellite rigid body are set to null. What is more, B2 is contained in the panel plane, so its initial sensitivity is null.

$$\boldsymbol{z}(\boldsymbol{q})^{\mathrm{T}} = \left(x_G\,,\, y_G\,,\, z_G\,,\, \psi\,,\, \theta\,,\, \varphi\,,\, x_{B2}\right)$$

$$\boldsymbol{z}_{q_0} = \begin{pmatrix} 0 & \dots & 1 & 0 & 0 & 0 & 0 & 0 & 0 \\ 0 & \dots & 0 & 1 & 0 & 0 & 0 & 0 & 0 \\ 0 & \dots & 0 & 0 & 1 & 0 & 0 & 0 & 0 \\ 0 & \dots & 0 & 0 & 0 & 1 & 0 & 0 & 0 \\ 0 & \dots & 0 & 0 & 0 & 0 & 1 & 0 & 0 \\ 0 & \dots & 0 & 0 & 0 & 0 & 0 & 1 & 0 \\ 0 & \dots & 0 & 0 & 0 & 0 & 0 & 0 & 1 \end{pmatrix} \quad , \quad \boldsymbol{z}_{\rho_0} = \begin{Bmatrix} 0 \\ \dots \\ 0 \\ 0 \\ 0 \\ 0 \\ 0 \\ 0 \\ 0 \end{Bmatrix} \tag{18}$$

SAT2. Similar to SAT1, but here B2 is out of the panel and the initial sensitivity of its x−coordinate is 4. Matrices defined for SAT1 apply to this case too except $\boldsymbol{z}_{\rho_0}$:

$$\boldsymbol{z}^{\mathrm{T}}_{\rho_0} = (0\,,\, \dots\,,\, 0\,,\, 0\,,\, 0\,,\, 0\,,\, 0\,,\, 0\,,\, 4) \tag{19}$$

Table 1
Five-bar mechanism. Summary of the test cases.

Case	Type	d (DOFs)	aram.	PIM	m_r	$d_s = d - m_r$ (SDOFs)
R1	Rigid	2	L_{A1}	Points 2 and 3 maintain their positions	0	2
R2	Rigid	2	L_{A1}	Point 3 maintains its position and 1 is horizontally displaced	0	2
R3	Rigid	2	L_{A1}	Point 3 maintains its position and point 1 is vertically displaced	0	2
F1	Flex.	5	L_{A1}	Bar 1–2 and both springs undeformed	5	0
F2	Flex.	5	L_{A1}	Bar 1–2 undeformed. Position of point 3 and angle α of bar A-1 respect to the horizontal are mantained	3	2
F3	Flex.	5	L_{A1}	Bar 1–2 and spring B-2 undeformed. Point 1 is vertically displaced.	4	1
F4	Flex.	5	L_{B1}	Bar 1–2 and both springs undeformed	5	0
F5	Flex.	5	L_{B1}	Bar 1–2 and spring B-2 undeformed. Point 1 maintains its position	4	1
F6	Flex.	5	L_{B1}	Bar 1–2 and spring B-1 undeformed. Angle α of bar 2–3 respect to the horizontal is maintained	4	1

Table 2
Four-panel satellite, definition of geometry, elastic properties and masses.

Body	General dimensions	Cross section	Mass	Material*
1 rigid body (satellite)	$2 \times 2 \times 2$ m	–	100 kg	–
4 torsional springs	Radius: 1 m	Type: circular, solid Area: 0.01 m^2	–	M1
8 panel beams	Length: 10 m	Type: circular, solid Area: 0.01 m^2	–	M2
4 rigid bars	Length: 2 m	–	0.1 kg	–
4 diagonal beams	Length: 10.198 m	Type: circular, solid Area: 10^{-5} m^2	–	M2

* $E = 1$ GPa, $\nu = 0.3$. Density of M1: 1 kgm^{-3}. Density of M2: 100 kgm^{-3}

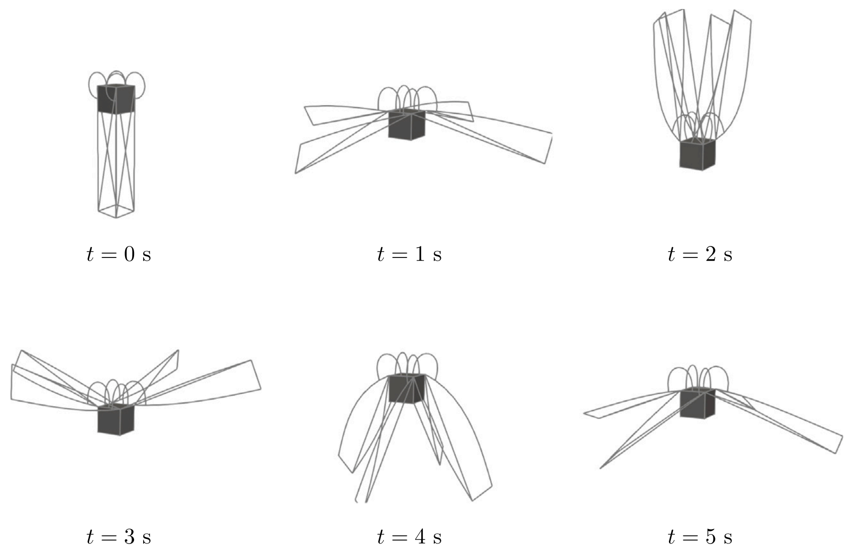

Fig. 11. Deployment manuver in a four-panel satellite: snapshots of the nominal movement.

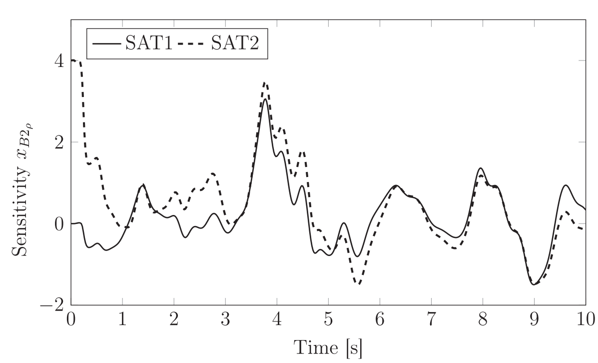

Fig. 12. Sensitivity of the $x-$ coordinate of point $B2$ with respect to the length of the rigid bar $B1 - B2$.

Fig. 12 shows the evolution of the sensitivity of the $x-$coordinate of point $B2$ with respect to the length of the rigid bar $B1 - B2$ for both PIMs. It is observed that, despite the different initial values, both curves tend to converge, due to the large numerical dissipation introduced by the integrator. This effect was far less visible in the five-bar example where the trapezoidal rule was employed, which is second-order accurate and introduces small numerical dissipation (in fact, exactly null for linear problems).

4. A formulation for including initially-rigid flexible bodies

This section contains a detailed formulation of the additional constraints $\boldsymbol{\Lambda}(\boldsymbol{q})$, introduced in the previous section, that are necessary to add when the associated PIM contains undeformed flexible bodies. It is assumed that they are already discretized by some means, such as the Finite Element Method with isoparametric elements, resulting in nodes

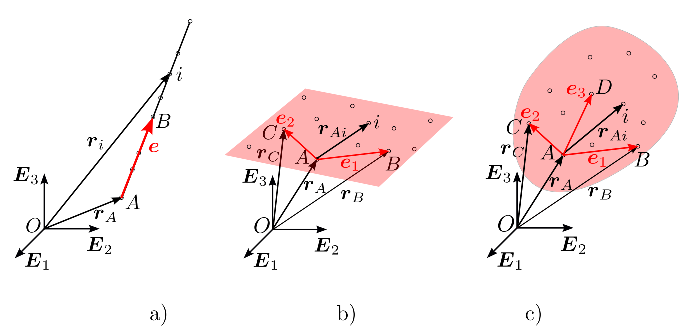

Fig. 13. a) 1D body; b) 2D body; c) 3D body.

whose coordinates are global Cartesian. Analogous formulations could be elaborated for other types of coordinates (e.g., natural, ANCF, etc.) but this is out of the scope of this paper.

4.1. *One-dimensional body (embedded in a 3D space) (Fig. 13(a))*

We first select two points A, B (that may not be the end points of the body) to define the non-unit vector $\boldsymbol{e} = \boldsymbol{r}_B - \boldsymbol{r}_A = \boldsymbol{r}_{AB}$. The total number of (Cartesian) coordinates of the $2+n_p$ points, with $n_p \geq 0$, is $n = 3(2+n_p)$, grouped in vector $\boldsymbol{q} = (\boldsymbol{r}_A, \boldsymbol{r}_B, \boldsymbol{r}_1, \dots, \boldsymbol{r}_{n_p})^{\mathrm{T}} \in \mathbb{R}^n$. On the other hand, the number of constraints is $m = 1 + 3n_p$, namely:

- 1 constant distance scalar constraint between A and B:

$$\Lambda_0 = \boldsymbol{e}^2 - L_{AB}^2 \tag{20}$$

- $3n_p$ scalar constraints enforcing that each point i is aligned with $\boldsymbol{e}$:

$$\boldsymbol{r}_{Ai} = c_i \boldsymbol{e} \quad \rightarrow \quad \boldsymbol{\Lambda}_i = \boldsymbol{C}_i \boldsymbol{q} \quad , \quad i = 1, .., n_p$$

$$\text{with} \quad \boldsymbol{C}_i = \begin{pmatrix} (c_i - 1)\mathbf{1}\,,\ -c_i\mathbf{1}\,,\ \mathbf{0}\,,\ \dots\,,\ \mathbf{0}\,,\ \underset{\substack{\uparrow \\ i}}{\mathbf{1}}\ ,\ \mathbf{0}\,,\ \dots\,,\ \mathbf{0} \end{pmatrix}_{3\times n}$$

$$\text{and} \quad c_i = \frac{\boldsymbol{r}_{Ai} \cdot \boldsymbol{e}}{L_{AB}^2}\,, \tag{21}$$

$\mathbf{0}$ and $\mathbf{1}$ being the null and unit 3×3 matrices respectively. Thus, the number of DOFs is $d = n - m = 5$. A 2-node rigid bar is just the special case for $n_p = 0$.

4.2. Two-dimensional body (embedded in a 3D space) (Fig. 13(b))

We select 3 three non-aligned nodes A, B, C first, which define, in general, the non-orthonormal base $\boldsymbol{e}_1 = \boldsymbol{r}_B - \boldsymbol{r}_A$, $\boldsymbol{e}_2 = \boldsymbol{r}_C - \boldsymbol{r}_A$. The cloud of $(3+n_p)$ points, with $n_p \geq 0$, belonging to the discretized body has a total of $n = 3(3+n_p)$ coordinates, grouped in vector $\boldsymbol{q} = (\boldsymbol{r}_A, \boldsymbol{r}_B, \boldsymbol{r}_C, \boldsymbol{r}_1, \dots, \boldsymbol{r}_{n_p})^{\mathrm{T}} \in \mathbb{R}^n$.

On the other hand, the number of constraints is $m = 3 + 3n_p$, namely:

- 3 constant distance scalar constraints among points A, B and C:

$$\boldsymbol{\Lambda}_0 = \left(\boldsymbol{e}_1^2 - L_{AB}^2\,,\ \boldsymbol{e}_2^2 - L_{AC}^2\,,\ (\boldsymbol{e}_2 - \boldsymbol{e}_1)^2 - L_{BC}^2\right)^{\mathrm{T}} \tag{22}$$

- $3n_p$ scalar constraints enforcing that any other point i is in the plane defined by $\boldsymbol{e}_1$ and $\boldsymbol{e}_2$:

$$\boldsymbol{r}_{Ai} = c_{i_1}\boldsymbol{e}_1 + c_{i_2}\boldsymbol{e}_2 \quad \rightarrow \quad \boldsymbol{\Lambda}_i = \boldsymbol{C}_i\boldsymbol{q} \quad \text{for} \quad i = 1, .., n_p \tag{23}$$

Thus, the number of DOFs is $d = n - m = 6$. The computation of each $3\times N$ matrix $\boldsymbol{C}_i$ requires the previous calculation of n_p vectors $\boldsymbol{c}_i = (c_{i_1}, c_{i_2})^{\mathrm{T}}$ with the expressions:

$$\boldsymbol{G}\boldsymbol{c}_i = \boldsymbol{b}_i, \text{ with} \quad \boldsymbol{G} = \begin{pmatrix} \boldsymbol{e}_1^2 & \boldsymbol{e}_1 \cdot \boldsymbol{e}_2 \\ \text{symm} & \boldsymbol{e}_2^2 \end{pmatrix} \text{ and } \quad \boldsymbol{b}_i = \begin{Bmatrix} \boldsymbol{r}_{Ai} \cdot \boldsymbol{e}_1 \\ \boldsymbol{r}_{Ai} \cdot \boldsymbol{e}_2 \end{Bmatrix} \tag{24}$$

where metric matrix $\boldsymbol{G}$ only needs to be computed once for all for the body. With vectors $\boldsymbol{c}_i$, final matrices $\boldsymbol{C}_i$ take the form:

$$\boldsymbol{C}_i = \begin{pmatrix} (c_{i_1} + c_{i_2} - 1)\mathbf{1}\,,\ -c_{i_1}\mathbf{1}\,,\ -c_{i_2}\mathbf{1}\,,\ \mathbf{0}\,,\ \dots\,,\ \mathbf{0}\,,\ \underset{\substack{\uparrow \\ i}}{\mathbf{1}}\ ,\ \mathbf{0}\,,\ \dots\,,\ \mathbf{0} \end{pmatrix}_{3\times n} \tag{25}$$

4.3. Three-dimensional body (Fig. 13(c))

The procedure begins by selecting 4 points A, B, C, D non-coplanar and non-aligned in groups of three, that define a general non-orthonormal basis $\boldsymbol{e}_1 = \boldsymbol{r}_B - \boldsymbol{r}_A$, $\boldsymbol{e}_2 = \boldsymbol{r}_C - \boldsymbol{r}_A$, $\boldsymbol{e}_3 = \boldsymbol{r}_D - \boldsymbol{r}_A$. The cloud of $(4 + n_p)$ points, with $n_p \geq 0$, has a total of $n = 3(4 + n_p)$ coordinates grouped in vector $\boldsymbol{q} = (\boldsymbol{r}_A, \boldsymbol{r}_B, \boldsymbol{r}_C, \boldsymbol{r}_D, \boldsymbol{r}_1, \dots, \boldsymbol{r}_{n_p})^{\mathrm{T}} \in \mathbb{R}^n$.

On the other hand, there are $m = 6 + 3n_p$ constraints, namely:

- 6 constant distance scalar constraints among A, B, C and D:

$$\begin{aligned} \boldsymbol{\Lambda}_0 = &\left(\boldsymbol{e}_1^2 - L_{AB}^2\,,\ \boldsymbol{e}_2^2 - L_{AC}^2\,,\ \boldsymbol{e}_3^2 - L_{AD}^2\,,\right. \\ &\left.(\boldsymbol{e}_2 - \boldsymbol{e}_1)^2 - L_{BC}^2\,,\ (\boldsymbol{e}_3 - \boldsymbol{e}_1)^2 - L_{BD}^2\,,\ (\boldsymbol{e}_3 - \boldsymbol{e}_2)^2 - L_{CD}^2\right)^{\mathrm{T}} \end{aligned} \tag{26}$$

- $3n_p$ scalar constraints enforcing that any other point i lies in the plane defined by $\boldsymbol{e}_1, \boldsymbol{e}_2$ and $\boldsymbol{e}_3$:

$$\boldsymbol{r}_{Ai} = c_{i_1}\boldsymbol{e}_1 + c_{i_2}\boldsymbol{e}_2 + c_{i_3}\boldsymbol{e}_3 \quad \rightarrow \quad \boldsymbol{\Lambda}_i = \boldsymbol{C}_i\boldsymbol{q} \quad \text{for} \quad i = 1, .., n_p \tag{27}$$

Thus, the number of degrees of freedom is $d = n - m = 6$. Similarly to the two-dimensional body, the computation of each $3 \times n$ matrix $\boldsymbol{C}_i$ requires the previous calculation of n_p vectors $\boldsymbol{c}_i = (c_{i_1}, c_{i_2}, c_{i_3})^{\mathrm{T}}$ with:

$$\boldsymbol{G}\boldsymbol{c}_i = \boldsymbol{b}_i\,, \quad \text{with} \quad \boldsymbol{G} = \begin{pmatrix} \boldsymbol{e}_1^2 & \boldsymbol{e}_1 \cdot \boldsymbol{e}_2 & \boldsymbol{e}_1 \cdot \boldsymbol{e}_3 \\ \text{symm} & \boldsymbol{e}_2^2 & \boldsymbol{e}_2 \cdot \boldsymbol{e}_3 \\ \text{symm} & \text{symm} & \boldsymbol{e}_3^2 \end{pmatrix} \quad \text{and} \tag{28}$$

$$\boldsymbol{b}_i = \begin{Bmatrix} \boldsymbol{r}_{Ai} \cdot \boldsymbol{e}_1 \\ \boldsymbol{r}_{Ai} \cdot \boldsymbol{e}_2 \\ \boldsymbol{r}_{Ai} \cdot \boldsymbol{e}_3 \end{Bmatrix}\,,$$

leading to the following final expression for $\boldsymbol{C}_i$:

$$\boldsymbol{C}_i = \begin{pmatrix} (c_{i_1} + c_{i_2} + c_{i_3} - 1)\mathbf{1},\ -c_{i_1}\mathbf{1},\ -c_{i_2}\mathbf{1},\ -c_{i_3}\mathbf{1},\ \mathbf{0},\ \dots,\ \mathbf{0},\ \underset{\substack{\uparrow \\ i}}{\mathbf{1}}\ ,\ \mathbf{0},\ \dots,\ \mathbf{0} \end{pmatrix}_{3\times n} \tag{29}$$

Remark 4.1. The proposed procedure defines constraints that are at most quadratic, which are very convenient from the implementation point of view.

5. Conclusions

Sensitivity analysis is a fundamental enabler for efficient gradient-based design optimization of flexible multibody systems. While comprehensive frameworks exist for computing sensitivities of the dynamic response using methods like DDM and AVM, a critical but often overlooked aspect is the computation of initial sensitivities, which are the derivatives of the initial state (positions and velocities) with respect to the design parameters.

The literature frequently treats the computation of these initial sensitivities as a mere implementation detail, lacking detailed explanation. This can pose a significant challenge in practice, as accurately determining these values is crucial for initiating the time integration of sensitivity equations and ensuring the correctness of the computed gradients for optimization.

This paper underscores and illustrates the importance of this specific problem in FMBS sensitivity analysis. In addition, a systematic analysis for computation of initial sensitivities in flexible systems is developed, with the aim of bridging the literature gap and providing a more streamlined approach to this crucial step. A small but representative example has been thoughtfully studied illustrating the significant impact that it has on the evolution of the sensitivities over time and, in all probability, on the overall optimization process.

CRediT authorship contribution statement

Juan C. García Orden: Writing – review & editing, Writing – original draft, Visualization, Validation, Supervision, Software, Resources, Project administration, Investigation, Funding acquisition, Formal analysis, Data curation, Conceptualization. **Juan J. Arribas Montejo:** Writing – review & editing, Validation, Software, Data curation, Conceptualization. **Álvaro López Varela:** Writing – review & editing, Validation, Methodology, Investigation, Conceptualization.

Declaration of competing interest

The authors declare that they have no known competing financial interests or personal relationships that could have appeared to influence the work reported in this paper.

Acknowledgements

The authors wish to acknowledge the financial support by the Spanish Ministerio de Ciencia, Innovación y Universidades (MICIU) as part of project PID2020-120270GB-C22 (Métodos de integración consistentes y elementos finitos no lineales para el análisis de sensibilidad de la dinámica de mecanismos flexibles) and project PID2020-120270GB-C21 (Diseño y control óptimo desistemas multi-cuerpo flexibles basado en análisis de sensibilidad de formulaciones con sistema de referencia flotante) and the financial support by MICIU/AEI/10.13039/501100011033/FEDER, UE of project PID2024-158324OB-I00 (Optimal design of military equipment based on flexible multibody dynamics with impact loads).

Appendix A

A.1. Detailed calculation of initial position sensitivities for R1

The constraints $\mathbf{\Phi}(\boldsymbol{q}) \in \mathbb{R}^4$, enforcing the constant-distance between points A-1, 1-2, 2–3 and 3-B, and the definition $\boldsymbol{z}(\boldsymbol{q})$ of the SDOFs are:

$$\mathbf{\Phi}(\boldsymbol{q}) = \left\{ \begin{array}{c} x_1^2 + z_1^2 - L_{A1}^2 \\ (x_2 - x_1)^2 + (z_2 - z_1)^2 - L_{12}^2 \\ (x_3 - x_2)^2 + (z_3 - z_2)^2 - L_{23}^2 \\ (x_3 - 1)^2 + (z_2)^2 - L_{3B}^2 \end{array} \right\} \quad , \quad \boldsymbol{z}(\boldsymbol{q}) = \left\{ \begin{array}{c} z_2 \\ x_3 \end{array} \right\} \tag{A.1}$$

With vector $\boldsymbol{z}_{\rho_0}$ given by (11), the system of equations (8) is in this case, for $\rho = L_{A1}$:

$$\begin{pmatrix} \mathbf{\Phi}_{\boldsymbol{q}_0} \\ \boldsymbol{z}_{\boldsymbol{q}_0} \end{pmatrix} \boldsymbol{q}_{\rho_0} = \left\{ \begin{array}{c} -\mathbf{\Phi}_{\rho_0} \\ \boldsymbol{z}_{\rho_0} \end{array} \right\} \tag{A.2}$$

$$\begin{pmatrix} 2x_{1_0} & 2z_{1_0} & 0 & 0 & 0 & 0 \\ -2(x_{2_0} - x_{1_0}) & -2(z_{2_0} - z_{1_0}) & 2(x_{2_0} - x_{1_0}) & 2(z_{2_0} - z_{1_0}) & 0 & 0 \\ 0 & 0 & -2(x_{3_0} - x_{2_0}) & -2(z_{3_0} - z_{2_0}) & 2(x_{3_0} - x_{2_0}) & 2(z_{3_0} - z_{2_0}) \\ 0 & 0 & 0 & 0 & 2(x_{3_0} - 1) & 2z_{3_0} \\ 0 & 0 & 0 & 1 & 0 & 0 \\ 0 & 0 & 0 & 0 & 1 & 0 \end{pmatrix} \boldsymbol{q}_{\rho_0} = \left\{ \begin{array}{c} 2L_{A1} \\ 0 \\ 0 \\ 0 \\ 0 \\ 0 \end{array} \right\} \tag{A.3}$$

$$\begin{pmatrix} -2 & -2 & 0 & 0 & 0 & 0 \\ -3 & 2 & 3 & -2 & 0 & 0 \\ 0 & 0 & -3 & -2 & 3 & 2 \\ 0 & 0 & 0 & 0 & 2 & -2 \\ 0 & 0 & 0 & 1 & 0 & 0 \\ 0 & 0 & 0 & 0 & 1 & 0 \end{pmatrix} \boldsymbol{q}_{\rho_0} = \left\{ \begin{array}{c} 2\sqrt{2} \\ 0 \\ 0 \\ 0 \\ 0 \\ 0 \end{array} \right\} \quad \rightarrow \quad \boldsymbol{q}_{\rho_0} = \left\{ \begin{array}{c} -0.5657 \\ -0.8485 \\ 0 \\ 0 \\ 0 \\ 0 \end{array} \right\} \tag{A.4}$$

A.2. Detailed calculation of initial position sensitivities for F1

Original constraints $\mathbf{\Phi}(\boldsymbol{q}) \in \mathbb{R}^3$ (from rigid bars A-1, 2–3 and 3-B) and additional constraints $\mathbf{\Lambda}(\boldsymbol{q}) \in \mathbb{R}^5$ (3 from rigidized beam 1-4-2 and two from rigidized springs B-1 and B-2) are:

$$\mathbf{\Phi}(\boldsymbol{q}) = \left\{ \begin{array}{c} x_1^2 + z_1^2 - L_{A1}^2 \\ (x_3 - x_2)^2 + (z_3 - z_2)^2 - L_{23}^2 \\ (x_3 - 1)^2 + (z_2)^2 - L_{3B}^2 \end{array} \right\}, \mathbf{\Lambda}(\boldsymbol{q}) = \left\{ \begin{array}{c} (x_2 - x_1)^2 + (z_2 - z_1)^2 - L_{12}^2 \\ -\frac{x_1}{2} - \frac{x_2}{2} + x_4 \\ -\frac{z_1}{2} - \frac{z_2}{2} + z_4 \\ (x1 - 1)^2 + z_1^2 - L_{B1}^2 \\ (x2 - 1)^2 + z_2^2 - L_{B2}^2 \end{array} \right\} \tag{A.5}$$

Since $d_s = 0$, $\boldsymbol{z}(\boldsymbol{q}), \boldsymbol{z}_{\boldsymbol{q}_0}, \boldsymbol{z}_{\rho_0}$ and $\dot{\boldsymbol{z}}_{\rho_0}$ do not appear in the formulation and the system of Eq. (8) results:

$$\begin{pmatrix} \mathbf{\Phi}_{\boldsymbol{q}_0} \\ \mathbf{\Lambda}_{\boldsymbol{q}_0} \end{pmatrix} \boldsymbol{q}_{\rho_0} = \left\{ \begin{array}{c} -\mathbf{\Phi}_{\rho_0} \\ -\mathbf{\Lambda}_{\rho_0} \end{array} \right\} \tag{A.6}$$

$$\begin{pmatrix} 2x_{1_0} & 2z_{1_0} & 0 & 0 & 0 & 0 & 0 & 0 \\ 0 & 0 & -2(x_{3_0}-x_{2_0}) & -2(z_{3_0}-z_{2_0}) & 2(x_{3_0}-x_{2_0}) & 2(z_{3_0}-z_{2_0}) & 0 & 0 \\ 0 & 0 & 0 & 0 & 2(x_{3_0}-1) & 2z_{3_0} & 0 & 0 \\ -2(x_{2_0}-x_{1_0}) & -2(z_{2_0}-z_{1_0}) & 2(x_{2_0}-x_{1_0}) & 2(z_{2_0}-z_{1_0}) & 0 & 0 & 0 & 0 \\ -\frac{1}{2} & 0 & -\frac{1}{2} & 0 & 0 & 0 & 1 & 0 \\ 0 & -\frac{1}{2} & 0 & -\frac{1}{2} & 0 & 0 & 0 & 1 \\ 2(x_{1_0}-1) & 2z_{1_0} & 0 & 0 & 0 & 0 & 0 & 0 \\ 0 & 0 & 2(x_{2_0}-1) & 2z_{2_0} & 0 & 0 & 0 & 0 \end{pmatrix} \boldsymbol{q}_{\rho_0} = \begin{Bmatrix} 2L_{A1} \\ 0 \\ 0 \\ 0 \\ 0 \\ 0 \\ 0 \\ 0 \end{Bmatrix} \tag{A.7}$$

$$\begin{pmatrix} -2 & -2 & 0 & 0 & 0 & 0 & 0 & 0 \\ 0 & 0 & -3 & -2 & 3 & 2 & 0 & 0 \\ 0 & 0 & 0 & 0 & 2 & -2 & 0 & 0 \\ -3 & 2 & 3 & -2 & 0 & 0 & 0 & 0 \\ -\frac{1}{2} & 0 & -\frac{1}{2} & 0 & 0 & 0 & 1 & 0 \\ 0 & -\frac{1}{2} & 0 & -\frac{1}{2} & 0 & 0 & 0 & 1 \\ -4 & -2 & 0 & 0 & 0 & 0 & 0 & 0 \\ 0 & 0 & -1 & -4 & 0 & 0 & 0 & 0 \end{pmatrix} \boldsymbol{q}_{\rho_0} = \begin{Bmatrix} 2\sqrt{2} \\ 0 \\ 0 \\ 0 \\ 0 \\ 0 \\ 0 \\ 0 \end{Bmatrix} \quad \rightarrow \quad \boldsymbol{q}_{\rho_0} = \begin{Bmatrix} 1.4142 \\ -2.8284 \\ 2.8284 \\ -0.7071 \\ 1.4142 \\ 1.4142 \\ 2.1213 \\ -1.7678 \end{Bmatrix} \tag{A.8}$$

Data availability

Data will be made available on request.

References

[1] Eberhard P, Schiehlen W. Computational dynamics of multibody systems: history, formalisms, and applications. J Comput Nonlinear Dyn 2005;1(1):3–12. https://doi.org/10.1115/1.1961875

[2] Shabana A. Dynamics of multibody systems. Wiley; 2013.

[3] Bauchau OA. Flexible multibody dynamics. Springer; 2011.

[4] Geradin M, Cardona A. Flexible multibody dynamics. A finite element approach. Wiley; 2001.

[5] Gufler V, Wehrle E, Zwölfer A. A review of flexible multibody dynamics for gradient-based design optimization. Multibody Syst Dyn 2021;53(4):379–409. https://doi.org/10.1007/s11044-021-09802-z

[6] Wang S, Tian Q, Hu H, Shi J, Zeng L. Sensitivity analysis of deployable flexible space structures with a large number of design parameters. Nonlinear Dyn 2021;105(3):2055–79. https://doi.org/10.1007/s11071-021-06741-4

[7] Dias JMP, Pereira MS. Sensitivity analysis of rigid-flexible multibody systems. Multibody Syst Dyn 1997;1(3):303–22. https://doi.org/10.1023/A:1009790202712

[8] Pi T, Zhang Y, Chen L. First order sensitivity analysis of flexible multibody systems using absolute nodal coordinate formulation. Multibody Syst Dyn 2012;27(2):153–71. https://doi.org/10.1007/s11044-011-9269-4

[9] Neto MA, Ambrósio JAC, Leal RP. Sensitivity analysis of flexible multibody systems using composite materials components. Int J Numer Methods Eng 2009;77(3):386–413. https://doi.org/10.1002/nme.2417

[10] Held A, Knüfer S, Seifried R. Structural sensitivity analysis of flexible multibody systems modeled with the floating frame of reference approach using the adjoint variable method. Multibody Syst Dyn 2017;40(3):287–302. https://doi.org/10.1007/s11044-016-9540-9

[11] Nejat AA, Moghadasi A, Held A. Adjoint sensitivity analysis of flexible multibody systems in differential-algebraic form. Comput Struct 2020;228:106148. https://doi.org/10.1016/j.compstruc.2019.106148

[12] Zhang M, Peng H, Song N. Semi-analytical sensitivity analysis approach for fully coupled optimization of flexible multibody systems. Mech Mach Theory 2021;159:104256. https://doi.org/10.1016/j.mechmachtheory.2021.104256

[13] Held A. On design sensitivities in the structural analysis and optimization of flexible multibody systems. Multibody Syst Dyn 2022;54(1):53–74. https://doi.org/10.1007/s11044-021-09800-1

[14] Wehrle E, Gufler V. Analytical sensitivity analysis of dynamic problems with direct differentiation of generalized-α time integration. Machines 2024;12(2). https://doi.org/10.3390/machines12020128

[15] Dopico D, Sandu A, Sandu C. Adjoint sensitivity index-3 augmented lagrangian formulation with projections. Mech Based Des Struct Mach 2022;50(1):48–78. https://doi.org/10.1080/15397734.2021.1890614

[16] Dopico D, Sandu A, Sandu C, Zhu Y. Sensitivity analysis of multibody dynamic systems modeled by ODES and daes. In Terze Z, editor. Multibody Dynamics, Vol. 35 of Computational Methods in Applied Sciences, Springer International Publishing; 2014. pp. 1–32. https://doi.org/10.1007/978-3-319-07260-9-1

[17] Dopico D, González F, Luaces A, Saura M, García-Vallejo D. Direct sensitivity analysis of multibody systems with holonomic and nonholonomic constraints via an index-3 augmented lagrangian formulation with projections. Nonlinear Dyn 2018. https://doi.org/10.1007/s11071-018-4306-y

[18] Dopico D, Zhu Y, Sandu A, Sandu C. Direct and adjoint sensitivity analysis of ordinary differential equation multibody formulations. J Comput Nonlinear Dyn 2014;10:011012. https://doi.org/10.1115/1.4026492

[19] Corner S, Sandu C, Sandu A. Modeling and sensitivity analysis methodology for hybrid dynamical system. Nonlinear Anal Hybrid Syst 2019;31:19–40. https://doi.org/10.1016/j.nahs.2018.07.003

[20] López Varela Á, Dopico Dopico D, Fernández AL. An analytical approach to the sensitivity analysis of semi-recursive ODE formulations for multibody dynamics. Comput Struct 2025;308:107642. https://doi.org/10.1016/j.compstruc.2024.107642

[21] García Orden JC, Cuenca Queipo J. A simple shear and torsion-free beam model for multibody dynamics. J Comput Nonlinear Dyn 2017;12(5):1–8. https://doi.org/10.1115/1.4036116

[22] García Orden JC. A conserving formulation of a simple shear- and torsion-free beam for multibody applications. Multibody Syst Dyn 2021;51:21–43. https://doi.org/10.1007/s11044-020-09754-w